

# Generation of polarisation-nonuniform modes in a high-power CO<sub>2</sub> laser

V.G. Niziev, V.P. Yakunin, N.G. Turkin

**Abstract.** A method describing radially and azimuthally polarised laser modes is presented, which is devoid of intrinsic contradictions and unjustified restrictions. The solutions of the wave equation found in the paper satisfy Maxwell's equation  $\nabla E = 0$ . This allowed the calculation of all the components of the fields of such modes, including the longitudinal one. Expressions for tight focusing of radially and azimuthally polarised modes are obtained in the Debye approximation. The methods of intracavity generation of such modes in a high-power industrial CO<sub>2</sub> laser are experimentally realised and methods of mutual transformation of these modes outside the cavity are developed. The intracavity generation of azimuthally polarised modes was achieved by using as a rear highly reflecting mirror either V-shaped axicons or metal diffraction mirrors with the relief period comparable to the wavelength. Radially polarised radiation was generated by using diffraction mirrors with the relief period of the order of two wavelengths. The polarisation-nonuniform TEM<sub>01</sub><sup>+</sup> and TEM<sub>11</sub><sup>+</sup> modes of power up to 1.8 kW are generated for the first time. In this case, the degree of polarisation was close to 100% within the entire radiation power range both in the near- and far-field zones. By using two half-wave phase shifters, the azimuthally polarised radiation is transformed to radially polarised radiation and vice versa, the energy efficiency of this transformation being 92%. These results open up the possibility for industrial applications of such radiation.

**Keywords:** radial and azimuthal polarisations, laser modes, diffraction mirrors, industrial CO<sub>2</sub> laser.

## 1. Introduction

The output radiation of most of the modern lasers is uniformly polarised. In this case, the ellipsometric parameters of radiation at all points of the laser beam cross

section are identical, while the field distribution in the beam cross section is described by the solution of the scalar wave equation (see, for example, [1]). In practice, as a rule, a laser resonator contains an element creating a certain polarisation of the output radiation, usually linear, with the specified direction of the field vector. To transform linear polarisation to circular, quarter-wavelength phase shifter is used outside the resonator of high-power industrial lasers in setups for laser cutting of metals.

Laser radiation polarisation considerably affects the results of laser processing of materials in many technological applications. In the case of linear polarisation, the efficiency and quality of metal processing (cutting and welding) depend on the polarisation direction. This disadvantage is absent in the case of circular polarisation, but circular polarisation is not optimal from the point of view of maximal absorption and minimal losses.

At the same time there exists a large class of solutions of the vector wave equation describing polarisation-nonuniform modes (PNMs) with unique physical properties (Fig. 1). In these modes, one or several ellipsometric parameters are not constant in the beam cross section.

Of most practical interest are modes with radial and azimuthal polarisation directions, which have the axial symmetry of all beam parameters, including polarisation. This property of laser beams proves to be quite useful for

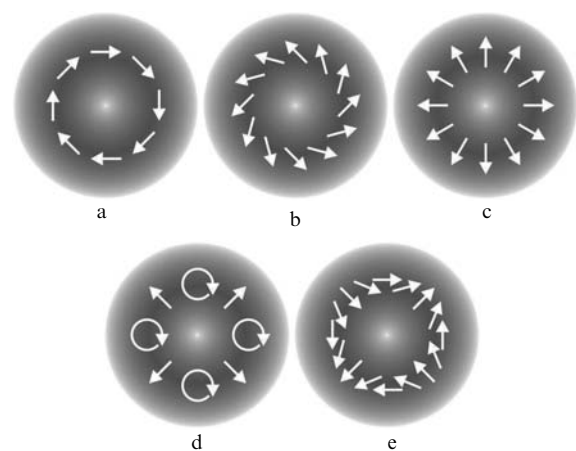


**Figure 1.** Types of polarisation-nonuniform modes: (a) azimuthally polarised; (b) with a constant angle between the field vector and radius; (c) radially polarised; (d) with polarisation type changing from point to point in the beam cross section; (e) linearly polarised with a complex topology of the vector field.

V.G. Niziev, V.P. Yakunin Institute on Laser and Information Technologies, Russian Academy of Sciences, ul. Svyatoozerskaya 1, 140700 Shatura, Moscow region, Russia; e-mail: niziev@mail.ru, YVP\_laser@inbox.ru;

N.G. Turkin State Research Center of the Russian Federation, Troitsk Institute for Innovation and Fusion Research, 140092 Troitsk, Moscow region, Russia; e-mail: turkin@triniti.ru

Received 19 August 2008; revision received 25 November 2008

Kvantovaya Elektronika 39 (6) 505–514 (2009)

Translated by M.N. Sapozhnikov

many applications in holography, interferometry, spectroscopy, photochemistry, and accelerator technology. In particular, laser beams polarised in the radial direction can be used for metal cutting, where the maximum absorption of laser radiation by the processed metal surface is required. An azimuthally polarised laser beam has minimal losses during radiation transfer along a hollow circular metal waveguide [2].

There exist two methods for obtaining axially polarised radiation – intracavity and outside the cavity.

In the first case, axially symmetric polarisation-selective optical elements are used in the cavity such as a conic Brewster window [3] or a conic reflector as a highly reflecting resonator mirror. It is convenient to use diffraction mirrors with the high local polarisation selectivity. Their special relief provides the maximum  $Q$  factor of a mode with the specified, for example, azimuthal direction of polarisation. In this case, other modes are suppressed due to strong intracavity losses. This method is preferable for high-power lasers, which usually have the high gain in the active medium, the low  $Q$  factor of the resonator, and relatively low spatial quality of radiation. This method is very convenient for lasers emitting at long wavelengths, for example, CO<sub>2</sub> lasers. Because the period of relief lines is proportional to the wavelength, it is much simpler to manufacture diffraction mirrors for CO<sub>2</sub> lasers than for visible lasers.

## 2. Theoretical description of laser modes with radial and azimuthal polarisations

The schemes illustrating the principles of formation of PNMs in the form of radially and azimuthally polarised beams are well known [2] (Fig. 2).

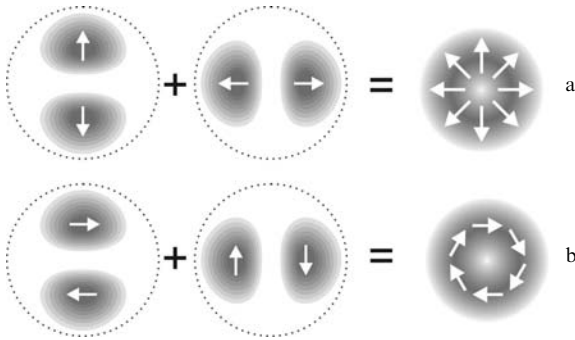


**Figure 2.** Formation of radially (a) and azimuthally (b) polarised modes due to a superposition of pairs of linearly polarised TEM<sub>01</sub> modes.

However, the theoretical description of PNMs based on these schemes with the use of classical solutions for the uniformly polarised Laguerre–Gaussian modes is very inefficient [1]. Problems appear that are related to serious intrinsic contradictions of classical solutions. The application of these solutions to PNMs drastically reduces the significance of such analysis.

It is well known that solutions of the scalar wave equation do not satisfy Maxwell's equation  $\nabla \mathbf{E} = 0$  [4], which makes impossible the formal and rigorous determination of the field of applications of this approximation. Classical solutions also contain other restrictions. The

solution of the scalar wave equation is valid only for a plane wave front, but not for a real laser beam having divergence. Classical solutions also neglect the longitudinal component of the field, which does not follow automatically from the paraxial approximation, being an additional restriction. A fundamental conclusion that Maxwell's equations do not admit, generally speaking, the decomposition of solutions into components seems quite certain. In this sense, azimuthal fields with the axial symmetry are the only exclusion.

### 2.1 Paraxial approximation in cylindrical coordinates

Consider radially or azimuthally polarised beams as the most interesting cases of PNMs. We will use the theoretical description of these beams by the method devoid of intrinsic contradictions and unjustified approximations.

We will use below only the spatial part of expressions for magnetic and electric fields, by using the substitution  $\mathbf{E}(r, \varphi, z, t) \rightarrow \mathbf{E}(r, \varphi, z) \exp(-i\omega t)$ ,  $\mathbf{H}(r, \varphi, z, t) \rightarrow \mathbf{H}(r, \varphi, z) \times \exp(-i\omega t)$  ( $r, \varphi, z$  are cylindrical coordinates), which is commonly applied in the description of wave processes.

By using the wave equation, we should solve a pair of equations for the field (magnetic or electric). For example, the equations

$$\Delta \mathbf{H} + k^2 \mathbf{H} = 0, \quad \nabla \mathbf{H} = 0$$

for a magnetic field.

We will seek the solution, for example, for a magnetic azimuthally directed field. It was proved in [5] that the condition of the radial (or azimuthal) direction of the field vector gives automatically the axial symmetry of the field amplitude distribution. Let us represent the required function in the form  $\mathbf{H} = H_\varphi(r, z) \mathbf{e}_\varphi$ , where  $\mathbf{e}_\varphi$  is the unit azimuthal vector. Such a representation satisfies the equation  $\nabla \mathbf{H} = 0$ , and the vector wave equation is reduced to the scalar equation of the form

$$\frac{1}{r} \frac{\partial}{\partial r} \left( r \frac{\partial H_\varphi}{\partial r} \right) + \frac{\partial^2 H_\varphi}{\partial z^2} + \left( k^2 - \frac{1}{r^2} \right) H_\varphi = 0.$$

We will seek the solution in the paraxial approximation, by separating the slowly varying field component  $H_\varphi(r, z) \rightarrow H_\varphi(r, z) \exp(ikz)$ . The solution of this scalar wave equation is known, and its mathematical derivation (in a more general form) can be found, for example, in [1]. In our case, this is the  $\rho - z$  part of the expression for Laguerre–Gaussian modes with the azimuthal index  $q = 1$ :

$$H_\varphi = \left( \frac{2p!}{\pi(p+1)!} \right)^{1/2} \frac{1}{w} (\sqrt{2}R) L_p^1(2R^2) \times \exp(-R^2) \exp(-i\theta), \quad (1)$$

where

$$\theta = 2(p+1) \arctan Z - ZR^2 - 2Z \frac{z_0^2}{w_0^2}; \quad R = \frac{r}{w};$$

$$Z = \frac{z}{z_0}; \quad z_0 = \frac{\pi w_0^2}{\lambda}; \quad w^2 = w_0^2(1 + Z^2);$$

$$L_p^1(x) = \sum_{m=0}^p (-1)^m \frac{(p+1)!}{(p-m)!(m+1)!} x^m;$$

$\lambda$  is the radiation wavelength;  $w_0$  is the fundamental mode beam radius; and  $p$  is the radial index.

The electric field components  $E_r$  and  $E_z$  are determined from Maxwell's equation  $\nabla \times \mathbf{H} = -ik\mathbf{E}$ . In the general form the analytic expressions for  $E_r$  and  $E_z$  are rather cumbersome, and therefore we write them only in the waist  $z = 0$ :

$$E_r(r, z = 0) \approx H_\varphi(r, z = 0) = \frac{2}{\sqrt{\pi}} \frac{1}{(p+1)^{1/2}} \frac{1}{w_0} \times R_0 L_p^1(2R_0^2) \exp(-R_0^2), \quad (2)$$

$$E_z(r, z = 0) = i \frac{1}{\pi\sqrt{\pi}} \frac{\lambda}{w_0} \frac{1}{w_0} (p+1)^{1/2} \exp(-R_0^2) \times [L_p(2R_0^2) + L_{p+1}(2R_0^2)]. \quad (3)$$

Here,  $L_p$  is the Laguerre polynomial,  $R_0 = r/w_0$ , and the approximate equality for  $E_r$  and  $H_\varphi$  takes place under the condition  $\lambda^2(\pi^2 w_0^2)^{-1} \ll 1$ .

The method for calculating a mode with the azimuthally directed magnetic field presented above cannot be formally applied to the radially directed field. Indeed, the solution of the form  $\mathbf{H} = H_r(r, z)\mathbf{e}_r(\varphi)$  does not satisfy the equation  $\nabla \mathbf{H} = 0$ . From the physical point of view this means that a mode with the azimuthally directed field (in the absence of other components of this field) exists, whereas a mode with the radially directed field is absent. This method allows one to calculate the field components for modes of two classes:

$$\mathbf{H} = H_\varphi(r, z)\mathbf{e}_\varphi(\varphi), \quad \mathbf{E} = E_r(r, z)\mathbf{e}_r(\varphi) + E_z(r, z)\mathbf{e}_z,$$

$$\mathbf{E} = E_\varphi(r, z)\mathbf{e}_\varphi(\varphi), \quad \mathbf{H} = H_r(r, z)\mathbf{e}_r(\varphi) + H_z(r, z)\mathbf{e}_z,$$

where  $\mathbf{e}_z$  and  $\mathbf{e}_r$  are the unit longitudinal and radial vectors.

The system of two equations, the wave equation and  $\nabla \mathbf{E} = 0$  (for the electric field) is additive. This means that a superposition of such modes with arbitrary complex coefficients also corresponds to Maxwell's equations.

## 2.2 Longitudinal field component

In connection with the study of PNMs of special interest is the field component directed along the propagation vector of an electromagnetic wave. This direction contradicts the transverse nature of the electromagnetic wave, and therefore this component is called the longitudinal one, and the energy related to it is not transferred. One of the approximations of the classical theory concerning paraxial beams is the neglect of this field component. However, in the case of tightly focused PNMs such a neglect is justified neither from the physical nor mathematical points of view because the longitudinal field component has the maximal amplitude where the 'usual' field component is zero. By now the first experiments on the detection of this component were already preformed [6, 7]. The longitudinal component of the electric field can be used to accelerate relativistic electrons [8, 9].

An analysis of the expressions presented above revealed several specific features of the longitudinal field component parallel to the wave vector:

(i) The maximum of this field is located on the beam axis, where the magnetic field and the radial component of the electric field are zero.

(ii) The field has an additional factor determining its smallness order  $\lambda/w_0$  compared to  $H_\varphi$  and  $E_r$ .

(iii) The imaginary unit in the expression for  $E_z$  suggests that this field component changes in time with the quarter-wavelength phase shift with respect to the magnetic field. As a result, the time-averaged Poynting vector, related to this longitudinal field component, is zero and this component does not transfer energy.

The explanation [7] of the physical features of this component by the absence of a magnetic field on the beam axis is inaccurate. The magnetic field and the longitudinal component of the electric field have overlapping distributions along the radius, however, according to the expression obtained, the time-averaged Poynting vector related to the longitudinal field component is zero at all the points of the beam-waist cross section. The physical nature of this component is as follows. Let a spatially restricted beam propagate along the  $z$  axis. Such a beam is converging or diverging. The components of wave vectors parallel to the  $z$  axis are directed to one side, they are added and form a travelling wave. The components of wave vectors perpendicular to the  $z$  axis are directed along the radius and form a standing wave with the field directed along the  $z$  axis. After the intersection with the  $z$  axis, the components of wave vectors perpendicular to the  $z$  axis form a diverging wave behind the beam waist. Figure 3 presents the distributions of  $H_\varphi$  and  $E_z$  for radially polarised R-TEM<sub>*p*1\*</sub> modes with  $p = 0, 1, 2$ .

## 2.3 Debye approximation for tight focusing

The calculation method described above should be also extended to the Debye approximation used to calculate fields in the focal plane of a lens upon tight focusing [10–13]. The calculation of the distribution for the azimuthally polarised component has no intrinsic contradictions and the results of the calculation satisfy Maxwell's equation  $\nabla \mathbf{E} = 0$ . The solution obtained, for example, for the magnetic field  $H_\varphi(r, z)$  allows one to calculate the radial and longitudinal components of the electric field:

$$E_r = \frac{1}{ik} \frac{\partial H_\varphi}{\partial z}, \quad E_z = i \frac{1}{kr} \frac{\partial(rH_\varphi)}{\partial r}.$$

Let us present the expressions for the field components in this case:

$$\begin{aligned} H_\varphi(r, z) &= k \int_0^\theta H_{\varphi 0}(f \sin \alpha) \sqrt{\cos \alpha} J_1(kr \sin \alpha) \\ &\quad \times \exp(ikz \cos \alpha) \sin \alpha \, d\alpha, \\ E_r(r, z) &= k \int_0^\theta H_{\varphi 0}(f \sin \alpha) \sqrt{\cos \alpha} J_1(kr \sin \alpha) \\ &\quad \times \exp(ikz \cos \alpha) \sin \alpha \cos \alpha \, d\alpha, \\ E_z(r, z) &= ik \int_0^\theta H_{\varphi 0}(f \sin \alpha) \sqrt{\cos \alpha} J_0(kr \sin \alpha) \\ &\quad \times \exp(ikz \cos \alpha) \sin^2 \alpha \, d\alpha. \end{aligned} \quad (4)$$

Here,  $\theta$  is the angle determined by the beam aperture and the focal distance  $f$  of the lens; and  $J_0$  and  $J_1$  are the Bessel

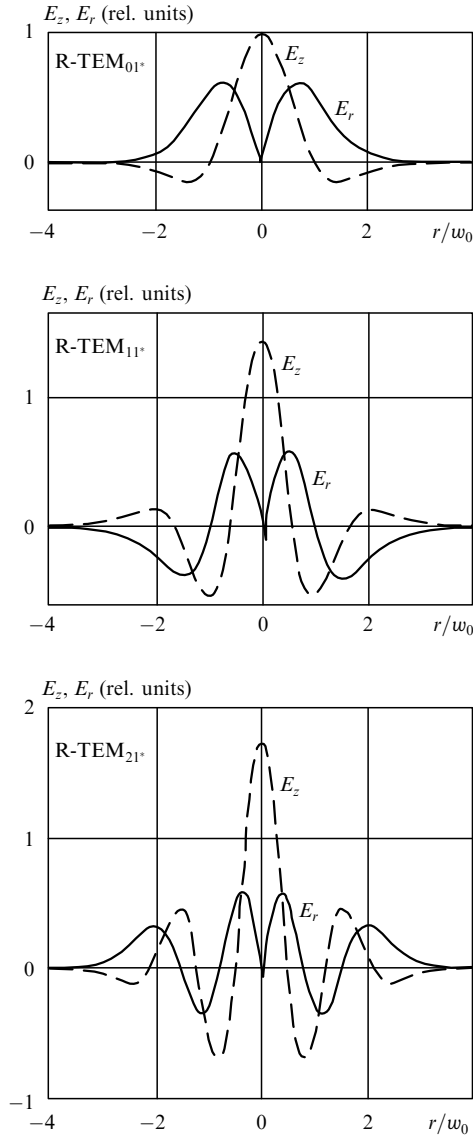


**Figure 3.** Distributions of electric field components  $E_z$  and  $E_r$  calculated by expressions (2) and (3) in the beam waist for radially polarised modes of different orders. The scales for  $E_z$  and  $E_r$  are mutually matched.

functions. The distribution of the fields in the beam waist corresponds to the condition  $z = 0$ . Similar expressions can be also written for the field components  $E_\varphi(r, z)$ ,  $H_r(r, z)$ , and  $H_z(r, z)$ . In this case, the azimuthally polarised field  $E_{\varphi 0}(r)$  is used as the initial field. The use of the Debye approximation for linearly or radially polarised radiation leads to the formal contradiction with the equation  $\nabla \mathbf{E} = 0$ .

The calculations of modes with axially symmetric polarisation presented above are physically correct and mathematically exact. Let us point out some practically important results of these calculations, which were used and can be used in experiments with such modes.

(i) The axial symmetry of polarisation determines the axially symmetric, circular (with the field zero at the centre) field amplitude distribution. Such a field distribution is absent in the class of uniformly polarised modes, and therefore the degree of radial (azimuthal) polarisation, which is experimentally measured below, also characterises the degree of the uniformity of the field distribution along the ring.

(ii) There exists a family of modes with axially symmetric polarisation which differ by their radial index  $p$ . The number of rings in a mode is  $p + 1$ .

(iii) In the case of tight focusing (the Debye approximation), the longitudinal field component is comparable in magnitude with the radial component and can play an important role in practical applications. The longitudinal field is formed by the superposition of waves with the antiparallel components of wave vectors.

### 3. Experimental generation of radially and azimuthally polarised modes in a high-power CO<sub>2</sub> laser

It is well known the polarisation of radiation considerably affects the parameters of laser metal cutting and welding [14–16]. At present in all commercial CO<sub>2</sub> laser metal cutting machine tools the circular polarisation of radiation is used at which processing parameters are independent of the laser beam propagation direction. The angle of incidence of radiation on the metal surface on the channel walls during laser cutting is close to 80°–90°, and, according to the Fresnel relation, absorption of circularly polarised radiation is approximately 50 % of the maximum possible value corresponding to the absorption of the P wave. In the case of radial polarisation, absorption in the channel walls is maximal, while for azimuthal polarisation it is minimal.

As mentioned above, methods, in which diffraction mirrors with the high local polarisation selectivity are used, occupy a particular place among the methods for generating modes with the axially symmetric polarisation in high-power lasers. A special line profile of diffraction mirrors provides the maximal  $Q$  factor for one mode, whereas other modes, having considerable intracavity losses, are suppressed.

The first experimental study on the generation of radially polarised radiation in a high-power industrial CO<sub>2</sub> laser with the use of a diffraction mirror was performed at the Institute of Problems of Laser and Information Technologies, RAS [17, 18].

We present below the results of experiments on the generation and mutual transformation of radially and azimuthally polarised modes in a high-power stable cavity industrial CO<sub>2</sub> laser. These experiments open up the possibility of investigations of the interaction of laser beams with chaotic, linear, circular, azimuthal, and radial polarisations with metals and the determination of technologies in which the use of such beams is most efficient.

#### 3.1 Diffraction mirrors and axicons for generating radiation with axially symmetric polarisation

The polarisation selectivity of diffraction gratings has long been known. The gratings themselves and their manufacturing technology are described in detail in [19], where it was proposed to use them for laser beam splitting. Another idea [20] was to use gratings with the high polarisation selectivity to generate linearly polarised radiation with a certain polarisation direction. The parameters of diffraction gratings were calculated by using the theory proposed in [21]. A metal-coated diffraction grating with a line period of 12 μm used in a industrial CO<sub>2</sub> laser in our experiments was fabricated by the photolithographic method with the liquid etching of copper. Radiation was incident on the grating

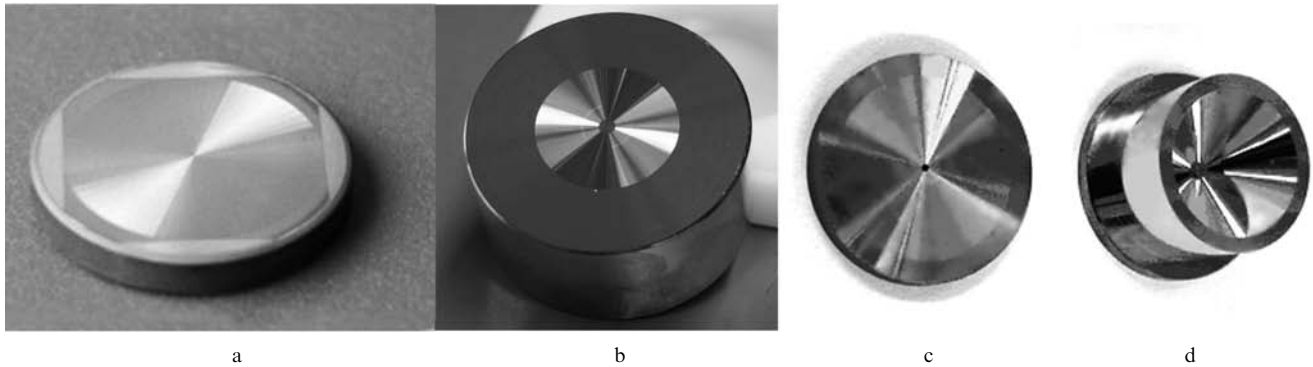


**Figure 4.** Diffraction mirrors (a–c) and axicon (d) for generating laser radiation with axially symmetric polarisation, fabricated by photolithography and chemical etching (IPLIT, RAS, 1998) (a); by diamond turning with the deposition of a gold coating (II–VI, USA) (b) and diamond turning (LIMO, Germany) (c, d).

normally to its surface, and the degree of polarisation of the 2.3-kW output radiation was 98.5%.

A mirror used in experiments [17] is shown in Fig. 4a. The parameters of diffraction lines and manufacturing technology of the grating were as in [21], but the line shape was adapted to generate radially polarised radiation. The 0.2- $\mu\text{m}$ -thick adhesion titanium layer and the 0.65- $\mu\text{m}$ -thick copper layer were deposited by the cathode evaporation method on a silicon substrate of diameter 50 mm. A trapezoid relief with specified parameters was produced by the photolithography method by using liquid etching. On the relief a protective reflection coating of total thickness 0.65  $\mu\text{m}$  was deposited. The profile parameters measured with a Talyster profilometer with an error of 0.2  $\mu\text{m}$  were: the height 0.65  $\mu\text{m}$ , the period 12  $\mu\text{m}$ , the top width 5.2  $\mu\text{m}$ , and the dip width 4.8  $\mu\text{m}$ . Because a high reflection coefficient is obtained for the electric field direction parallel to the lines, the shape of the lines for generation of radially polarised radiation was complex. The entire surface of the mirror was divided into 72 sectors, the lines in each sector being parallel to the bisector of the sector angle. The reflection coefficient  $\rho_{\parallel}$  for radiation at 10.6  $\mu\text{m}$  for the electric field vector parallel to lines was 94%, and for the wave with the electric field vector perpendicular to lines it was  $\rho_{\perp} = 72\%$ . This diffraction mirror was used as a highly reflecting resonator mirror.

In the last years great progress has been made in the manufacturing technology of diffraction mirrors with complicated line profiles. Now the diamond turning of diffraction mirrors is used instead of complicated multistage photolithography and etching technologies (Figs 4b, c).

Azimuthally polarised radiation can be generated either by using a diffraction mirror or an axicon (Fig. 4d). The axicon has both advantages and disadvantages. The manufacturing technology of axicons is somewhat simpler and does not require complicated calculations, however, the polarisation selectivity of the axicon is lower. This is explained by the difference in the Fresnel reflection of the P and S waves from an inclined surface. The axicon cannot provide the generation of radially polarised radiation, however, due to its geometry it can stabilise the radiation pattern. If namely radially polarised radiation should be generated, it is necessary to use an additional device transforming the azimuthal polarisation to radial, which consists of two successive half-wavelength phase shifters.

A V-shaped 90° axicon with the base of diameter 36 mm used in our experiments was fabricated of highly pure copper by diamond turning. At the axicon centre a through hole (with the minimal possible diameter of 1.5 mm) for a cutter exit was located.

### 3.2 Experimental setup

Radially and azimuthally polarised radiation was generated in a industrial transverse gas-flow, transverse-discharge CO<sub>2</sub> laser. The five-pass laser resonator of length 8 m had a plane mirror and the output mirror with the radius of curvature 30 m. The fundamental mode beam radius was  $w_0 = 6.7$  mm. When usual mirrors were used, up to 2.5 kW of multimode radiation with a divergence of 2.3 mrad was generated. The optical scheme of the laser resonator is presented in Fig. 5. A conventional highly reflecting resonator mirror was replaced by a diffraction mirror or an axicon, which provided the maximal  $Q$  factor of the resonator for radially or azimuthally polarised modes. Radiation in the laser resonator is incident on folding mirrors M2 and M3 at an angle of no more than 1°, and therefore reflection from these mirrors is virtually isotropic with respect to polarisation. The output mirror is made of ZnSe. The calculated fundamental mode beam radius  $w_0$  on the rear mirror of this resonator was 6.7 mm, while the beam radius on the output mirror was 7.8 mm.

Figure 6 shows the scheme of measuring the energy, spatial, and polarisation characteristics of radiation under study. The output power of the CO<sub>2</sub> laser was measured with an OPHIR 4000W-CAL power meter. A KCl wedge beamsplitter reflected  $\sim 4\%$  of the beam power to the channel measuring the spatial distribution of the near- or



**Figure 5.** Scheme of the resonator of a industrial CO<sub>2</sub> laser: (M1) ZnSe output mirror with the radius of curvature  $R = 30$  m; (M2, M3) plane folding mirrors; (M4) polarisation-selective element (diffraction mirror or axicon).

far-field degree of polarisation. The far-field degree of polarisation was measured by placing into the measurement channel a lens with an aperture mounted in its focal plane. An MLR-1 polariser, consisting of two successively placed germanium plates oriented at the Brewster angle, was used to select the required linear polarisation. Radiation transmitted through the polariser was detected with an RK 5100 radiometer.

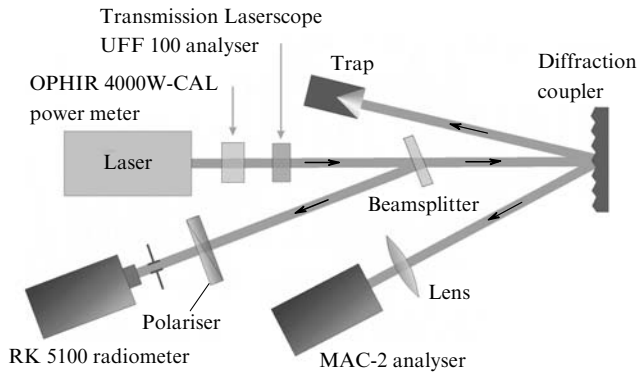


Figure 6. Scheme for measuring radiation characteristics.

The near-field radiation intensity distribution in the forward beam was detected with a Laserscope UFF100 power meter, while the far-field intensity distribution was detected with a MAC-2 Mode Computer Analyzer on which ~ 0.1 % of the incident radiation power was deflected by the diffraction grating.

By analysing radiation intensity distributions for different positions of the polariser axis, we determined the polarisation state of the beam and calculated the degree of polarisation. We also considered the near- and far-field radiation intensity distributions characterising the divergence and mode composition of radiation.

**3.3 Generation of azimuthally polarised radiation**

Azimuthally polarised radiation was generated with the help of a V-shaped, 90° axicon or a diffraction mirror. The relief lines had the trapezoid shape, the relief period was 12 μm, and its depth was 0.5 μm. The mirror was fabricated by diamond turning, the relief pattern representing concentric circles. The local polarisation selectivity was 5 %. The grating profile is presented in Fig. 7.

The typical near-field pattern of generated radiation on a ceramic screen is shown in Fig. 8a. The laser output power

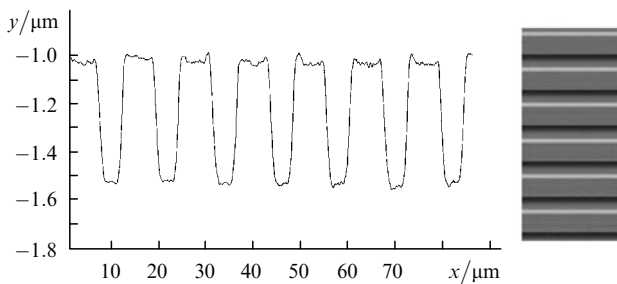


Figure 7. Profile of lines of a diffraction mirror for generating azimuthally polarised laser beam.

was measured to be 950 W, the distance to the laser being 16 m. The radiation intensity distribution measured in this cross section is shown in Fig. 8b, where the calculated radial intensity distribution

$$I(r) \sim \frac{r^2}{w^2} \exp\left(-2 \frac{r^2}{w^2}\right)$$

for the azimuthally polarised TEM<sub>01</sub> mode is also presented, which is in qualitative agreement with experimental results.

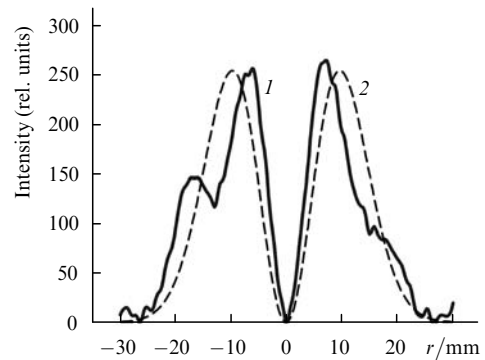
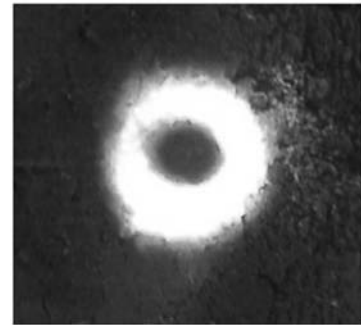


Figure 8. Radiation intensity distributions in the beam cross section at a distance of 16 m from a laser; the imprint of generated radiation on a ceramic screen (a) and experimental (1) and calculated (2) dependences (b). The radial distribution of the field is calculated by (2); the radiation intensity is  $I(r) = |E|^2$ .

The polarisation state in the forward beam was analysed with the help of a KCl plate oriented at the Brewster angle. The radiation intensity distribution in the beam reflected from the plate and observed on the screen clearly demonstrates the azimuthal orientation of the electric field vector of the light wave.

Figure 9 shows the typical radial distribution of the degree of polarisation  $\xi(r)$  measured in the beam cross section in the near-field zone. The degree of polarisation was calculated from the expression

$$\xi(r) = \frac{I_\varphi(r) - I_r(r)}{I_\varphi(r) + I_r(r)}$$

At all points of the beam where the radiation intensity was more than 15 % of the maximum intensity, the degree of polarisation  $\xi(r)$  achieved 96 % – 99 %, which corresponds to the excess of the azimuthally polarised radiation intensity over the radially polarised radiation intensity by 50 – 200 times. The accurate measurements of  $\xi(r)$  at the beam centre

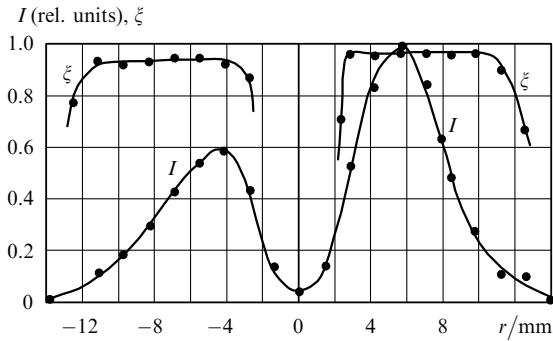


**Figure 9.** Near-field radial distributions of the intensity  $I(r)$  and degree of polarisation  $\xi(r)$ . The aperture diameter is 0.9 mm.

and at its edges were complicated because it was difficult to displace the aperture (Fig. 6) strictly along the beam diameter and also due to the intrinsic noise of the photo-detector during measuring low intensities.

The far-field intensity distributions (in the focal plane of a lens with  $f = 785$  mm) are shown in Fig. 10 in the absence of a polariser and also for selected horizontal and vertical polarisations.

These figures show clearly that the radiation intensity along the diameter directed along the direction of selected polarisation is close to zero. This means that the laser beam is indeed azimuthally polarised.

Azimuthally polarised radiation can be also obtained by the transformation of radial polarisation into azimuthal outside the resonator. A device that can be used to perform such (and inverse) transformation is described below.

### 3.4 Generation of radially polarised radiation

All the above-mentioned aspects related to the generation of azimuthally polarised radiation such as the degree of polarisation, the mode composition of the beam, etc. are also applied to the generation of a radially polarised laser beam.

The first study of the generation of radially polarised radiation in a high-power industrial CO<sub>2</sub> laser was performed in [17]. The laser radiation in the conventional resonator was nonpolarised. When a diffraction mirror was used, the laser generated predominantly radially polarised radiation of power up to 1.8 kW. The diffraction mirror was

fabricated by etching (see Fig. 4a); its parameters are presented in section 3.1. The calculated reflection coefficient of the diffraction mirror for the fundamental TEM<sub>00</sub> mode was 83.5%, which suggested that this mode was not completely suppressed, the more so the diffraction losses for this mode are minimal. This component of the laser beam is nonpolarised. We can assert that the increase in the polarisation selectivity of the diffraction mirror will reduce the intensity of the transverse modes of the laser. In experiments with the moderate selectivity performed in our study, the mode composition of radiation was reduced in fact to two modes: TEM<sub>00</sub> mode and the radially polarised TEM<sub>01</sub> mode. The radiation divergence decreased from 3.3 to 2.2 mrad, while the degree of polarisation of the laser beam was 50%.

Further experiments were performed with the diffraction mirror fabricated by diamond turning (see Fig. 4b). The mirror had a relief with a period of 18 μm of depth 5 μm (Fig. 11).

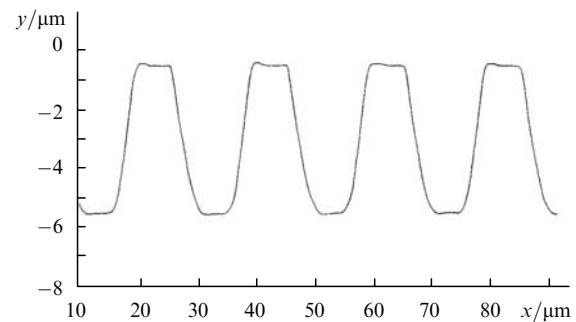


**Figure 11.** Profile of lines of a diffraction mirror for generating a radially polarised laser beam.

The imprint of generated radially polarised radiation on a ceramic screen is completely similar to the imprint of the azimuthally polarised beam (Fig. 8a).

The polarisation state in the forward beam was analysed with a KCl plate oriented at the Brewster angle. The intensity distribution in the beam reflected from the plate is shown in Fig. 12. Interference in Fig. 12 appears due to reflection of radiation from the two surfaces of the plate.

The far-field intensity distributions are shown in Fig. 13 for two directions of the polariser axis.

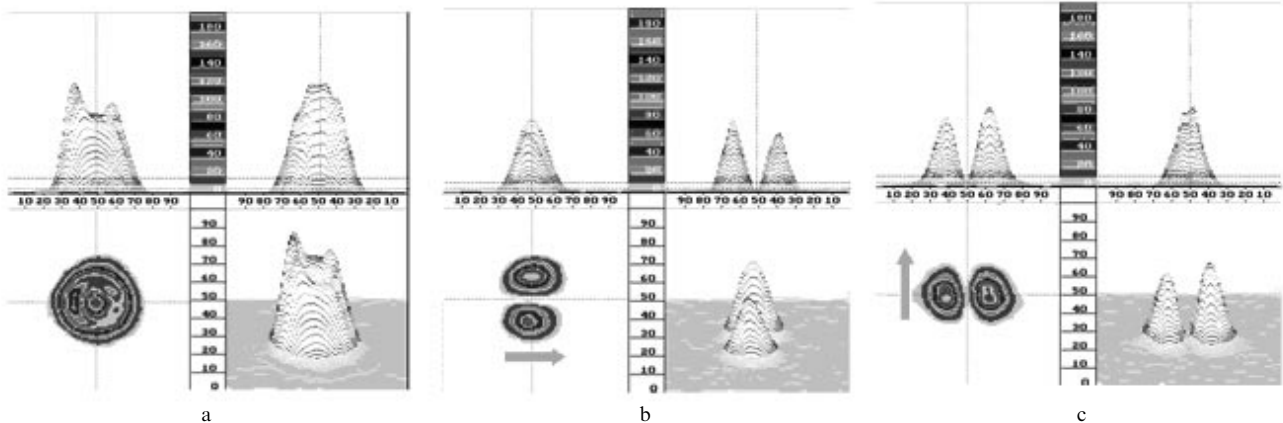


**Figure 10.** Far-field intensity distributions for azimuthally polarised radiation obtained with a MAC-2 analyser without a polariser (a) and for horizontal (b) and vertical (c) directions of its axis (shown by the arrows).

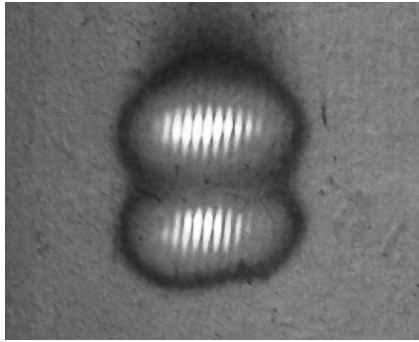


**Figure 12.** Intensity distribution in a beam reflected from a KCl plate oriented at the Brewster angle.

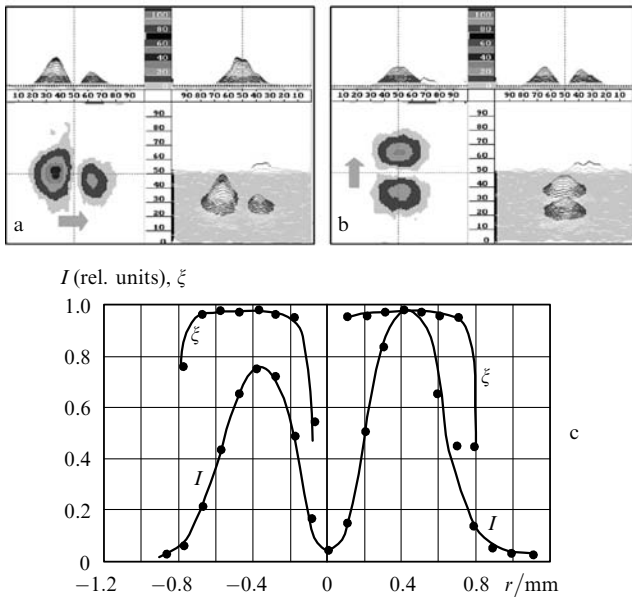


**Figure 13.** Far-field intensity distributions for radially polarised radiation obtained with a MAC-2 analyser at the horizontal (a) and vertical (b) directions of the polariser axis (shown by the arrows), and the far-field radial distributions of the intensity  $I(r)$  and degree of polarisation  $\xi(r)$  (c).

Figure 14 presents the far-field intensity distribution for the radially polarised  $TEM_{11^+}$  mode. This result, which was observed for the first time, was obtained in a three-pass resonator of length 4.8 m. The radiation power was 2 kW.

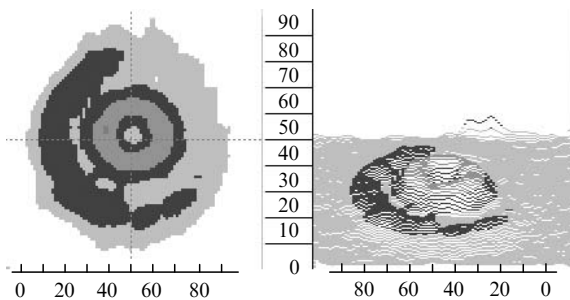


**Figure 14.** Far-field intensity distribution for the radially polarised  $TEM_{11^+}$  mode (cf. Fig. 3).

### 3.5 Transformation of axially symmetric polarisations outside the resonator

The idea of transformation of azimuthal polarisation to radial (and vice versa) proposed in [22] is based on the transmission of radiation through two half-wavelength phase shifter (Fig. 15). In this case, the electric field vector should turn by  $90^\circ$ . This occurs if the axes of phase shifters make the half-angle, i.e.  $45^\circ$ . In this case, the rotation angle of the field vector is independent of its initial orientation. This scheme is remarkable in a way that it allows the transformation of PNMs with the help of standard optical elements.

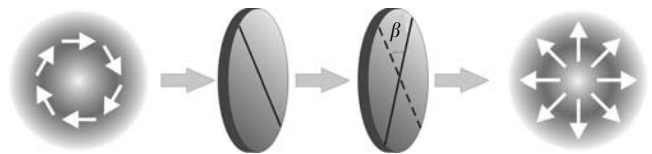


**Figure 15.** Scheme of the transformation of azimuthal polarisation to radial with the help of two half-wavelength phase shifters;  $\beta = 45^\circ$ .

Phase shifters used in high-power  $CO_2$  lasers represent either metal mirrors with proper coatings or diffraction gratings. However, such components providing the half-wavelength phase shift are not series-produced. At the same time, phase quarter-wavelength metal mirrors are widely used in laser metal cutting facilities. A combination of such mirrors allows the transformation of an azimuthally polarised beam to a radially polarised one.

The polarisation converter consists of three similar units (Fig. 16a). Each of the units contains a pair of parallel mirrors. The incident laser beam is directed at an angle of  $45^\circ$  to a mirror, and the output beam is parallel to the incident beam. The two units use phase quarter-wavelength mirrors, and as a result the unit operated as a half-wavelength phase shifter. These two units should be connected so that the planes of incidence of radiation on the first and second units should intersect at an angle of  $45^\circ$ .

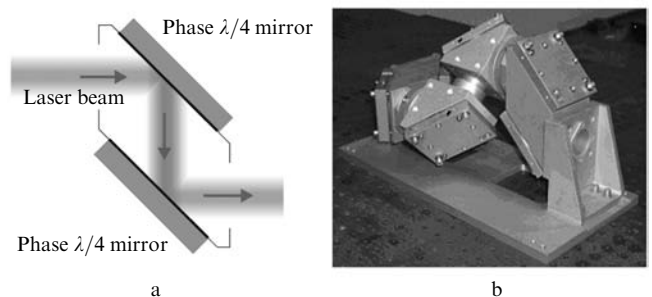


**Figure 16.** Scheme of one of the three units of a half-wavelength phase shifter (a) and the photograph of the assembled phase shifter.

The standard reflection coefficient of phase quarter-wavelength mirrors for the angle of incidence  $45^\circ$  is equal to 98 %, and therefore total losses of the transformation of one axially symmetric polarisation to another are  $\sim 8 \%$ . In this case, the laser beam is displaced in height, which is obviously inconvenient for the use of laser metal cutting machine tools.



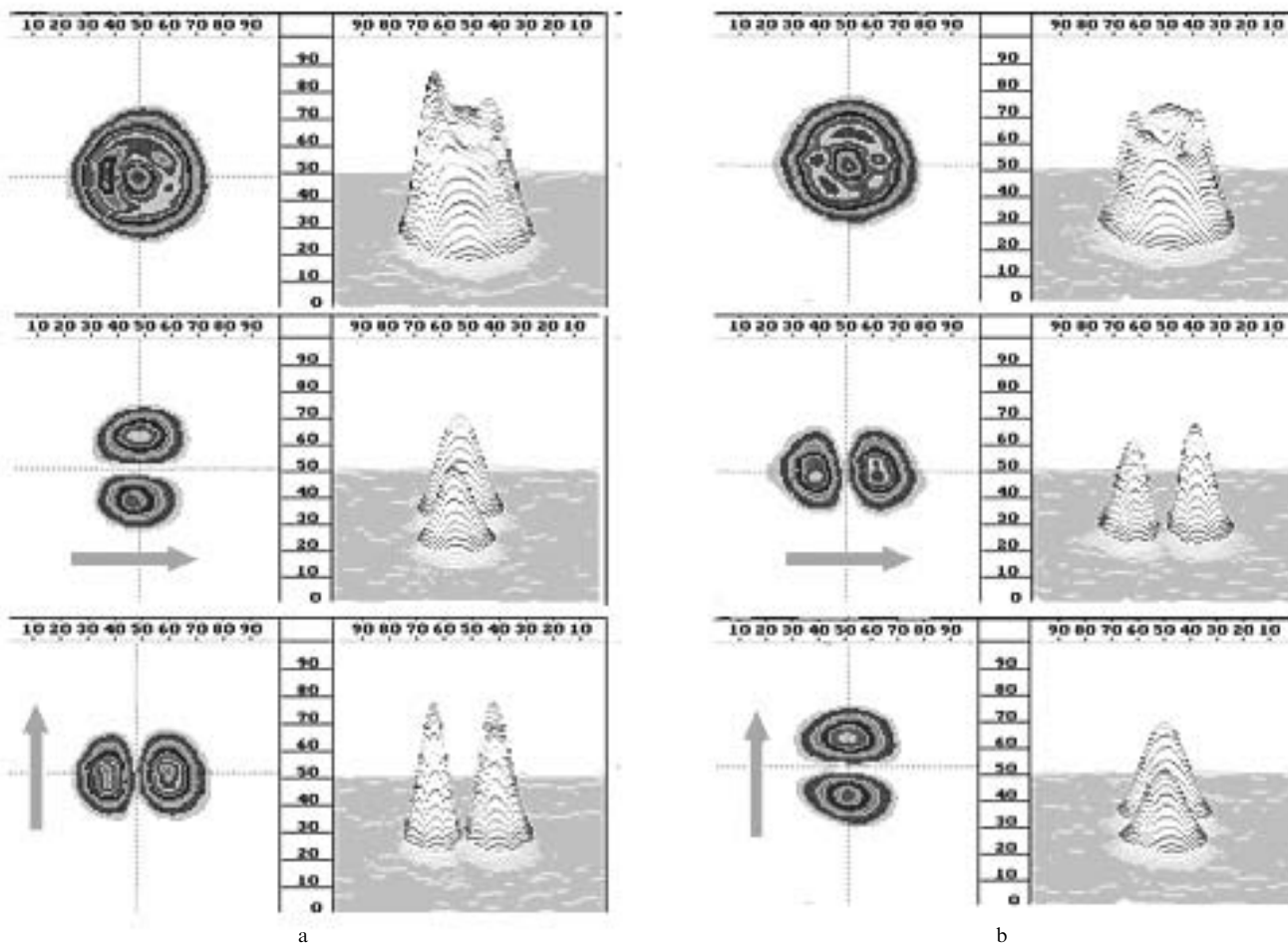


**Figure 17.** Intensity distributions for the azimuthally polarised mode in front of the converter (a) and for the radially polarised mode behind the converter (b). The arrows show the direction of the polariser – analyser axis.

The third unit contains usual mirrors and is used only to return the output beam to the direction of the incident beam. Total losses in the polarisation transformation by retaining the beam propagation direction are about 10 %.

Figure 17 presents the far-field intensity distributions for the initial azimuthally polarised beam and the output beam.

One can see that the intensity distributions in the beams for the same selected polarisation in front and behind the converter correspond to the beams with orthogonal electric field vectors at any point.

The results obtained in the study can be used for comparative investigations of the interaction of radiation with different polarisation states (chaotic, linear, circular, radial, and azimuthal) with metals during welding and cutting and also to analyse the interaction of laser beams with axially symmetric polarisation states with materials when the longitudinal components of the electric and magnetic fields appear upon tight focusing.

#### 4. Conclusions

We have calculated the electric and magnetic field components for radially and azimuthally polarised laser modes both in the paraxial approximation and in the case of tight focusing. The method used in the study is devoid of intrinsic contradictions and unjustified restrictions, and the solutions of the wave equation correspond to Maxwell’s equation  $\nabla E = 0$ .

By using the V-shaped axicon or polarisation-selective diffraction mirrors as a highly reflecting mirror, we have demonstrated intracavity methods for generating radially and azimuthally polarised modes in a high-power industrial CO<sub>2</sub> laser. Plane diffraction mirrors with trapezoid lines were fabricated by diamond turning. The degree of radiation polarisation has been measured by using these elements. The generation of radially and azimuthally polarised TEM<sub>01</sub><sup>\*</sup> and TEM<sub>11</sub><sup>\*</sup> modes of power up to 1.8 kW has been demonstrated for the first time. The degree of radiation polarisation in the near- and far-field zones was close to 100 %. The transformation of an azimuthally polarised beam to a radially polarised beam (and vice versa) was realised by using a pair of half-wavelength reflection phase shifters. The results obtained in the study open up the possibility of technological applications of radially and azimuthally polarised radiation.

#### References

1. Solimeno S., Crosignani B., Di Porto P. *Guiding, Diffraction, and Confinement of Optical Radiation* (New York: Acad. Press, 1986; Moscow: Mir, 1989).
2. Pressley R.J. (Ed). *Handbook of Laser with Selected Data on Optical Technology* (Cleveland: Chemical Rubber Comp., 1971).
3. Chen-Ching Shih et al. United States Patent No. 5.359.622 (1994).
4. Lax M., Louisell W.H., Mc Knight W.B. *From Maxwell to Paraxial Wave Optics Phys. Rev. A*, **11**, 1365-70 (1975).

5. Nesterov A.V., Niziev V.G. *J. Phys. D: Appl. Phys.*, **33**, 1817 (2000).
6. Dorn R., Quabis S., Leuchs G. *Phys. Rev. Lett.*, **91**, 233901 (2003).
7. Miyaji G., Miyanaga N., Tsubakimoto K., Sueda K., Ohbayashi K. *Appl. Phys. Lett.*, **84**, 3855 (2004).
8. Tidwell S.C., Ford D.H., Kimura W.D. *Appl. Opt.*, **29**, 2234 (1990).
9. Tidwell S.C., Kim G.H., Kimura W.D. *Appl. Opt.*, **32**, 5222 (1993).
10. Nesterov A.V., Niziev V.G. *J. Opt. B: Quantum and Semiclassical Opt.*, **3**, 215 (2001).
11. Stamnes J. *Waves in Focal Regions. The Adam Hilger Series on Optics and Optoelectronics* (Bristol: Institute of Phys. Publ., 1986).
12. Quabis S., Dorn R., Eberler M., Glockl O., Leuchs G. *Appl. Phys. B*, **72**, 109 (2001).
13. Kozawa Y., Sato S. *Opt. Lett.*, **31** (6), 820 (2006).
14. Garashchuk V.I., Kirei V.I., Shinkarev V.A. *Kvantovaya Elektron.*, **13**, 2515 (1986) [*Sov. J. Quantum Electron.*, **16**, 1660 (1986)].
15. Powell J. *CO<sub>2</sub>-Laser Cutting* (London: Springer-Verlag, 1993) p. 16.
16. John F. *Ready Handbook of Laser Material Processing* (Orlando, FL: Laser Institute of America, Magnolia Publ., Inc., 2001).
17. Nesterov A.V., Niziev V.G., Yakunin V.P. *J. Phys. D: Appl. Phys.*, **32**, 2871 (1999).
18. Yakunin V.P., Nesterov A.V., Niziev V.G. *Proc. SPIE Int. Soc. Opt. Eng.*, **3889**, 603 (1999).
19. Haidner H., Kipfel P., Sheridan J., Schwider J., Strebl N., Lindolf J., Collischon M., Lang A., Huttfless J. *Opt. Eng.*, **32** (8), 1860 (1991).
20. Yakunin V.P., Balykina E.A., Manankova G.I., Novikova L.V., Seminogov V.N., in *Abstracts, VI Mezhdunarodnaya Konf. 'Lazernye tekhnologii '98'* (VI International Conference on Laser Technologies-98) (Shatura, NITsTL, RAS, 1998) p. 68.
21. Okorkov V.N., Panchenko V.Ya., Russkikh B.V., Seminogov V.N., Sokolov V.I., Yakunin V.P. *Opt. Eng.*, **33** (10), 3145 (1994).
22. Niziev V.G., Nesterov A.V. *J. Phys. D: Appl. Phys.*, **32**, 1455 (1999).